INTERNATIONAL ATOMIC ENERGY AGENCY
UNITED NATIONS EDUCATIONAL, SCIENTIFIC AND CULTURAL ORGANIZATION
INTERNATIONAL CENTRE FOR THEORETICAL PHYSICS
I.C.T.P., P.O. BOX 586, 34100 TRIESTE, ITALY, CABLE CENTRATOM TRIESTE

H4.SMR/773-13

College on Medical Physics:
Radiation Protection and Imaging Techniques

5 - 23 September 1994

# *Physics of Radiological Imaging*

G.E. Gigante

Università degli Studi di Roma
"La Sapienza"
Dipartimento di Fisica
Roma

# PHYSICS OF RADIOLOGICAL IMAGING

*G.E. Gigante - Dipartimento di Fisica - Università di Roma "La Sapienza" - Piazzale A. Moro 2 - 00185 Roma*

**Index:**



## 1 *BASIC EXPERIMENTAL X RAY PHYSICS:* SOURCES AND DETECTORS

In the recent years is growing the interest of the other parts of the physical research for the x ray physics which is a traditional field of experimental physics having a strong influence in the applied physics and mainly in the medical physics. This interest is mainly due to the larger availability of new x ray detectors with interesting characteristics, like the position sensitive ones, and of new sources of high brillance, such as that of synchrotron radiation.

### 1.1Sources

The most important characteristics of an x ray source are: (i) the spectral distribution of the emitted photons[1]; (ii) the intensity of the source in terms of energy (or number of photons) emitted for unit solid angle and time[2]; (iii) the angular distribution of the emitted photons, i.e. the polar plot of the intensity.

[1] Some sources are monochromatic, such as some radioisotopic sources, i.e. they emit photons of only one energy



#### 1.1.1 The X ray Tube

One of the early applications of the x rays, in the first months after their discover by Röntgen, was the production of radiographic images. The most interesting feature of these image resides in the possibility to see inner parts of the imaged objects. Many of us remember the first radiograph the image of the hand of the Röntgen's wife with the ring. The November 5 1995 are hundred years that the x ray are available for the scientific community.

At that time the instrumentation was constituted of a Crookes tube (the father of the modern x ray tube) and a photographic film. These two devices are still in use in the modern radiography.

An x ray tube is an high voltage vacuum tube with an anode and a cathode, see fig.1; the electrons are strongly accelerated from the cathode to the anode and, being accelerated by a strong electric field produced by a $\Delta V$ of tenths of KV, impinge on the latter with a kinetic energy of thousand electron-volt (eV), .

$$\Delta V = \frac{1}{2} m_e v^2 \qquad (1)$$

where $m_e$ is the electron mass; the electrons impinging on the anode can be considered as monochromatic being their velocity at the start from the cathode negligible.

Entering the anode the primary electrons give rice mainly to three types of interactions: the scattering with the electrons of the target (ionization), the Rutherford scattering due to the coulumbian field of nuclei and the emission of photons during the deceleration of the primary electrons in the target (bremsstralhung). The energy edge for annihilation is well above that which can be reached by the electrons in a x ray tube[3]. There are other interactions but, for an electron (i.e. a charged particle characterized by a very large charge over mass ratio), their probabilities are very small.

Figure 1

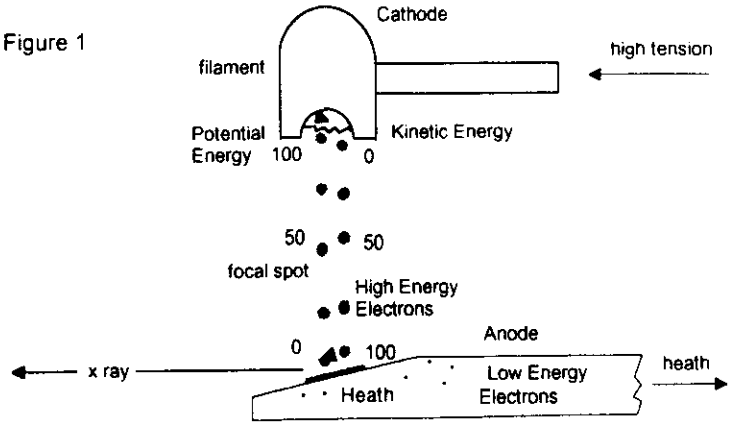


As a consequence of above mentioned interactions the x ray spectrum produced is not monoenergetic, showing the characteristic shape of figure 2. The most prominent characteristics of the spectrum are the occurrence of a maximum, a high

[2] It is possible, and common in dosimetry, define the photon fluence rate at a certain distance from the source in a given area (number of photons/ mm²-sec)

[3] In the case of linear accelerator for radiotherapy this edge is usually exceeded

energy limit which shifts toward higher energies as the applied voltage increases and the presence in the spectrum of the characteristic x ray lines of the target. The high energy limit (known as the Duane-Hunt limit) is given by the applied voltage, and is a direct consequence of the quantum nature of electromagnetic radiation, i.e., no photon can be emitted with an energy greater than that of the bombarding electrons. The absorption of the photons by the tube window and by the interposed filters determine the position of the maximum in the spectrum. The characteristic lines are a consequence of the ionization.

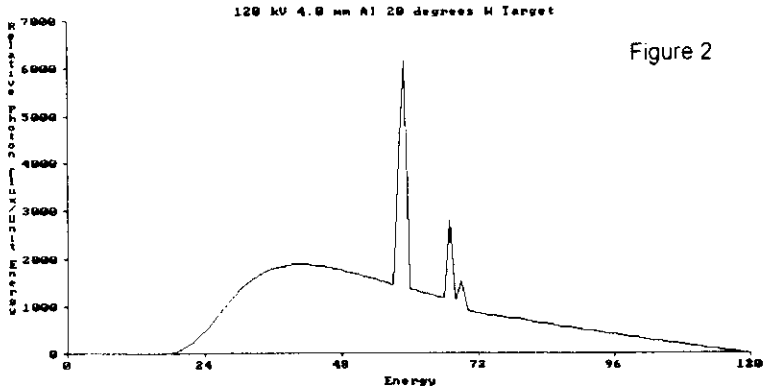


Figure 2

**Bremsstralhung**

Focusing our attention on the bremssrtalhung it is easy to note that this effect can be understood also from a classical point of view. In the development of electromagnetic theory it is established that an accelerated charge loses its energy progressively in the form of electromagnetic radiation, and an important situation arises when an electron is accelerated in the direction parallel to its motion. Let us consider a charge moving in the direction of x axis with an acceleration **a** and a point P (see figure 3) at a distance r having an angle θ with the x-axis, it is easy to observe that, in this point, the electric field E lies in the plane x-r and is perpendicular to r and the magnetic field **H** is perpendicular to it

$$|\mathbf{H}| = |\mathbf{E}| = \left(\frac{|\vec{a}|\, e}{r c^2}\right)\sin(\theta) \qquad (2)$$

The outward flow of energy associated with the acceleration is given by the Poynting vector **N**

$$\mathbf{N} = \frac{c}{4\pi}(\mathbf{E}\wedge\mathbf{H}) \quad |\mathbf{N}| = \frac{c}{4\pi}\left(\frac{|\vec{a}|\, e}{r c^2}\right)^2 \sin^2(\theta) \qquad (3)$$

The $\sin^2(\theta)$ term give rise to the familiar polar diagram for dipole radiation. It is well known that this equation is correct only when the velocity of the charge is small in comparison with c, i.e. $\beta = \frac{v}{c} << 1$ , in our case the primary electrons enter in the



target with a very high velocity $\beta \approx 1$ in this case the equation (3) must be substituted with

$$\mathbf{N} = \frac{c}{4\pi}\left(\frac{z\, e\, a}{r c^2}\right)^2 \frac{\sin^2(\theta)}{(1-\beta\cos(\theta))^6} \qquad (3')$$

Therefore for ß ~ 1 the radiation is strongly forward peaked, It is possible to demonstrate that for thin target the distribution is characterized by minima in forward and backward directions and a gradual movement of the maximum of intensity toward smaller angles as the electron energy is increased. For longer slowing down time, i.e., in the case of emission of lower energy photons, the angular distribution is less forward peaked; this is the case of electron opaque targets and this is the reason of the fact that in a x ray tube the electron beam impinges on the anode surface with a large incidence angle.

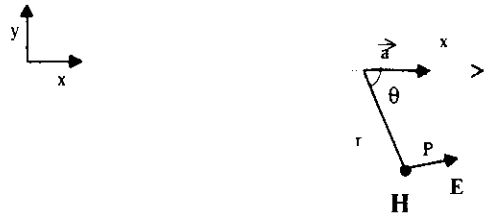


figure 3

Integrating the equation 3 over all angles we obtain the total intensity as a function of the acceleration

$$I = \int \mathbf{N} 2\pi r^2 \sin(\theta) d\theta = \frac{2(z\, e\, a)^2}{3c^3} \qquad (4)$$

That is, for a single charge, the Larmor formula. The Larmor formula, which can be used for calculating the energy irradiated by the electron during its interaction with the nucleus, is valid for non relativistic velocities, therefore, in order to use it in the case of a relativistic electron it is necessary to change the reference system from that of the nucleus (S) to that of the electron (S') . In this reference system the electron is at rest at time zero and its velocity remain small, in comparison with c, during the interaction with the nucleus. The acceleration to which is subjected the electron in S' is:

$$\left|\vec{a}\right| = \frac{\gamma z Z e^2}{m_e(b^2+(\beta c t)^2)} \qquad (5)$$

Where Z is the atomic number of the target and γ is the relativistic factor to be used in order to have the force in S'. The energy emitted in the system S', during the collision with the interaction parameter b, is given by:

$$w(b) = \int_{-\infty}^{\infty} I'(t')dt' = \frac{2z^2e^2}{3c^3}\int_{-\infty}^{\infty} a^2(t')dt' = \left(\frac{\pi}{3}\right)\frac{\gamma(z^2 Z\, e\, r_0)^2}{b^3} \qquad (6)$$

where $r_0 = \frac{e^2}{mc^2}$ is the classical radius of the electron and b, as shown in figure 4, is the impact parameter. It worth to note that an interaction with a small impact parameter (fig.5 a) give rise to a photon in the high energies part of the spectrum, whereas a weak collision, i.e. a large impact parameter (fig.5 b), give rise to a photon in the lower part of the spectrum.

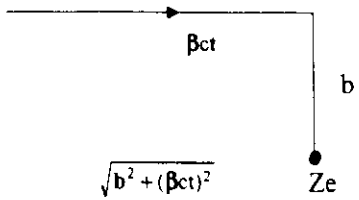


figure 4

Entering the target the electron is subjected to $2\pi nbdbdx$ interactions per unit path (dx) with b between b and b+db, being n the number of atoms for unit volume. Integrating equation for the impact parameters it is possible to show that,

$$\left(-\frac{dE}{dx}\right) = \int_{b_{min}}^{b_{max}} w(b) 2\pi\, nbdb = \frac{2\pi^2}{3}(z^2 Zer_0)^2 \gamma\, n \int \frac{db}{b^2} = \frac{2\pi^2}{3}(z^2 Zer_0)^2 \gamma\, n \left[\frac{1}{b_{min}} - \frac{1}{b_{max}}\right] \quad (7)$$

The result of this equation is the energy irradiated by the electron for unit path which is the integral of the emitted spectrum. Considering only energetic photons, i.e. x rays, $b_{min} \ll b_{max}$ therefore $1/b_{max}$ can be neglected. It is easy to demonstrate that the impact parameter is related to the time for which the electron is subjected to the acceleration during its passage across the nucleus field

$$\Delta t = \frac{2b}{\beta c}; \quad \Delta t' = \frac{2b}{\gamma\beta c}; \quad \text{therefeore} \quad \nu'_{max} = \frac{\gamma\beta c}{2b_{min}} \quad (8)$$

It is evident the photon energy ($h\nu_{max}$) cannot exceed that of the electron E and, being the duration of the pulse of x-radiation very small, it is a reasonable hypothesis that the spectrum, the Fourier transform of this pulse, is constant between zero and the maximum frequency. Under this hypothesis the energy irradiated in the energy interval $h\nu + h\nu + dE$ is given by:

$$\left(-\frac{dE}{dxdh\nu}\right) = \frac{\left(-\frac{dE}{dx}\right)}{h\nu_{max}} = \frac{4\pi^2}{3hc}(z^2 Zer_0)^2 n \quad (9)$$

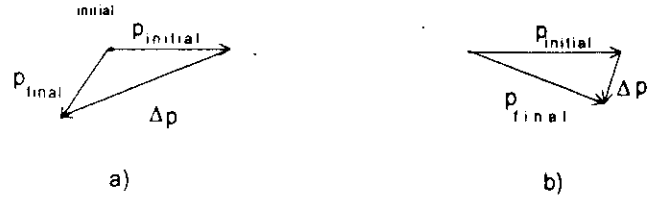


figure 5

Therefore, the energy irradiated in a spectral window by the electron in a dx path is constant and the number of photons in this energy window (dN) is:



$$\frac{dN}{d\nu} = \frac{1}{X_0 h\nu} \quad \text{with} \quad \frac{1}{X_0} = \frac{4\pi^2}{3hc}(z^2 Zer_0)^2 n \quad (10)$$

Treating the problem with quantum mechanics it is possible to verify that the equation 10 is true apart from a slowing varying factor F(E,E') that can be neglected in many cases. In figure 5 it is shown a typical bremsstralhung spectrum from a thin foil.

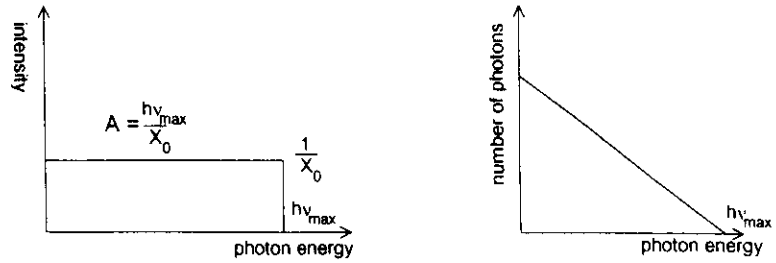


figure 6

The electrons entering the target loss progressively their energy; the above equations did not take into account of this fact. In other words the above written equations are valid only for the case of a thin target. It is easy to image that the average energy of the electron impinging on the surface is bigger than that of the electron in the inner parts of the target. Therefore these electrons will produce a bremsstralhung spectrum different from that of the impinging ones (see figure 7). The stopping power of an electron is given by the Bethe-Bloch formula that can be written as

$$\left(-\frac{dE}{dx}\right) \approx \frac{const}{E} \quad (11)$$

Substituting dx in the equation (9) it is easy to show that:

$$I(\nu) \propto E_0 - E = h\nu_{max} - h\nu \quad (12)$$

It is obvious the fact that the high energy part of the irradiated spectrum is produced near the surface of the target . The number of photons N emitted in the spectral window $h\nu + h\nu + dE$, is

$$N(\nu) \propto \frac{(h\nu_{max} - h\nu)}{h\nu} \quad (13)$$

It is easy to demonstrate that the dependence of the intensity by the target atomic number (Z) is linear and the equation (13) can be written as

$$I(\nu) = \text{const.} \times Z \times (h\nu_{max} - h\nu) \quad (14)$$

The dependence of the bremsstralhung from the charged particle mass can be deduced substituting in the equation 5 the mass of the electron with that of an heavier particle (M). In this case the particle in the nucleus field is subjected to a lower acceleration, therefore the emitted radiation is reduced by a factor $(\frac{m_e}{M})^2$, that for a proton is $(\frac{1}{1840})^2 \approx 3 \times 10^{-6}$.

**Summary:**

The bremsstralhung spectrum produced by an electron beam traversing a thin layer of material is continuous with equal intensity for unit energy (fig.6). However, if

the beam, entering the anode, traverse a thickness that is much more larger than the mean free path of the electron in the material, the spectrum shows a linear decrease of the intensity with the photon energy (fig.7). In fact, the bremsstralhung produced in the layer immediately below the surface have proportionally less photon of high energy than the first one because some electrons have been partially decelerated and the mean energy of the beam is smaller. The electron impinging on the target is characterized by a relativistic velocity, consequently (equation 3) the emitted radiation is strongly forward peaked. Their velocity progressively decreases and the radiation becomes less forward peaked. In practice, an electron beam traversing a thick target produces a maximum of intensity in the forword direction. In particular, the position of this maximum depends from some parameters, such as the energy of the electrons and the material.

Figure 7

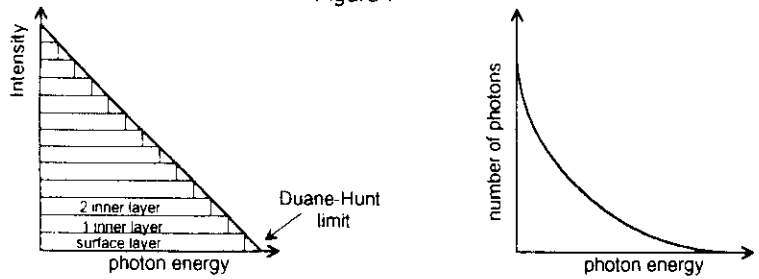


**Characteristic x ray lines**

The second kind of interaction, i.e. the ionization process, is a electron-electron scattering that removes one electron from an atom of the target and, with the re-equilibrium of the atom, gives rice to the production of the characteristic x ray lines of the elements of the anode. For example in the very common case of a tungsten anode the following x ray line will appear in the spectrum 69.09,67.20,59.31,57.97, 11.28, 9.96,9.67,8.40, 8.333 KeV when the electrons energy is larger than the binding energy of the corresponding tungsten sunshell; for example the characteristic K-lines (69.09,67.20,59.31 keV) will appear only when the tube voltage is more than 70 KV.

**Filters**

The decrease of the intensity toward the low energies is due to the absorption (inherent filtration) of the glass envelop, or the berillium window, of the vacuum tube . In many cases it is useful to place a thin sheet of an absorbing material after the window (added filtration). The absorption of the photons depends by the filter thickness and by the material constituting it, using an element of higher atomic number (or a more thick filter) the energy of the maximum of the tube spectrum will be shifted toward higher energies.

The absorption at an energy hv is given by the well known relation:

$$I = I_0 e^{-(\frac{\mu}{\rho})\rho x} = I_0 e^{-(\frac{\mu}{\rho})m} \qquad (15)$$



where $(\frac{\mu}{\rho})$ is the mass absorption coefficient of the filter and m is its the mass for unit surface. The mass absorption coefficient for the elements can be considered as the sum of three terms:

$$(\frac{\mu}{\rho}) = (\frac{\mu}{\rho})_{photo} + (\frac{\mu}{\rho})_{incoh} + (\frac{\mu}{\rho})_{coh} \qquad (16)$$

where $(\frac{\mu}{\rho})_{photo}$ is the photoelectric mass absorption coefficient, $(\frac{\mu}{\rho})_{incoh}$ is the incoherent scattering (Compton) mass absorption coefficient and $(\frac{\mu}{\rho})_{coh}$ is the coherent scattering mass absorption coefficient. The $(\frac{\mu}{\rho})_{photo}$ decreases rapidly ($E^{-3.24}$ ) with energy; this interaction, in fact, is dominant in the energy range of the binding energies of the inner electrons of the atoms. The coefficient is characterized by jumps in correspondence of the binding energies of the electrons; in the case of the binding energy of the K-shell it is common to speak of K-edge. Using a correct element it is possible to place this K-edge in the energy interval of interest; in some applications, in which a source with a quasimonochromatic spectrum is necessary, it is useful to use a couple of K-edge filters in order to select an energy interval. The x ray spectrum after the filtration appears as that shown in figure 8.

Figure 8

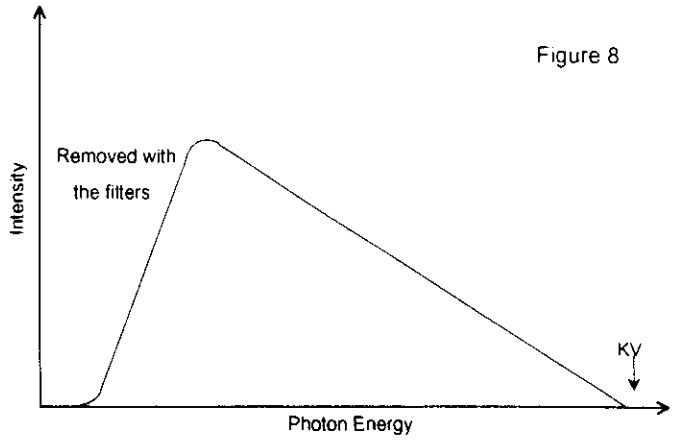


1.1.2 Synchrotron Radiation sources and other x ray sources

There are others sources, less common than the x ray tube. In particular, are available many radioisotopic x ray sources emitting x ray lines or continuous spectra. These sources are used for radiographic studies of large absorbing objects (γ-graphie), but are not valid alternative to the x ray tube in the low and intermediate energy interval.

For radiography are now available small and large particle accelerators as linear accelerators and synchrotrons. Particular interest is actually devoted to the **synchrotron radiation** that constitutes a source of x rays nearly unique characteristics. As in the x ray tube the radiation is emitted during the acceleration of the electrons, in this case, in the bending magnets of the storage ring. If E is the energy of the electrons, expressed in GeV, and R is the radius of curvature of the electron orbit, a stationary observer will see a pulse of electromagnetic radiation when an electron bunch will

be deflected in the magnet. The electrons will radiate for a time of $\Delta t = 2(\frac{R}{c})(1-\beta^2)^{\frac{1}{2}}$; the duration of this pulse for stationary observer is shorter of a factor of $(1-\beta^2)$, it thus is

$$\Delta t = \frac{R}{c}(1-\beta^2)^{\frac{3}{2}} = \frac{R}{c}(\frac{mc^2}{E})^3 \qquad (17)$$

The pulses will recur with a frequency of the order $\frac{c}{2\pi R}$ and so the radiation will consist of a fundamental at this frequency and a series of harmonics up to a limit of the order

$$\nu_c = \frac{3c}{2R}(\frac{E}{mc^2})^3 \qquad (18)$$

That is the critical frequency, which devides the emitted power into equal halves. This radiation is strongly forward directed due to the relativistic velocity of the electrons, in the plane of the electron orbit the divergence of the beam is $\Delta\theta = \frac{E}{mc^2}$ that,in the case of a 1.5 GeV synchrotron, is 0.3 mradians. The harmonics are so closely spaced that the spectrum appears as continuous with a characteristic shape.

$$\frac{dI}{d\theta} = \frac{\sqrt{3}}{2\pi}\alpha\frac{E}{mc^2}\frac{\Delta\nu}{\nu}\frac{I}{e}G(\frac{\nu}{\nu_c}) = 2.457\times10^{13}E(GeV)I(A)G(\frac{\nu}{\nu_c}) \qquad (19)$$

where a is the fine-structure constant, $\frac{\Delta\nu}{\nu}$ is the bandwidth and I is the storage ring current; G is a function equal to one at the maximum that is at $\nu_c$.

The synchrotron radiation is polarized in the plane of the electron orbit and is elliptically polarized out of this plane.

### 1.2 Detectors.

There are many types of detectors for the energy interval of interest for the radiography (KeV's photons); unfortunately most of them are single detectors that can be hardly used in the detection of an image. In the table are listed the principal classes of x ray detectors with their principal characteristics such as their degree of energy and position sensitivity, energy resolution and spectral efficiency. It is evident that the detectors with a good energy resolution are characterized (unfortunately) by a low spatial resolution. Actually in the clinical use only few types of detectors are in use for radiology: the films, the screen-film systems, the image intensifier, the photostimulable screens, the scintillators (in the CT-scanners and in the absorptiometric systems). The solid state detectors are the most used in the research.

In this particular moment the detectors play a fundamental role in the development of the new digital radiography systems. In this sense some type of detectors can be classified as inherently analogic (films, screen-film systems) and others digital. The trend is to substitute the analogic detector with that digital which are more easily interfaced with a digital comouter; this process is started, but at this moment only a small fraction of the radiographic investigations are carried out with digital procedures. One limitation is in the high cost of digital systems that require larger costs to begin but (potentially) a lower costs for the operation and storage. A digital system, in fact, require a costly acquisition system and a computer for the elaboration and storage of data. The advantages for a radiologist are mainly in the better organization of the information (easier storage and retrieval) and in the possibility to elaborate (enhance and restore the image) and perform simultaneous reading of images taken with different modalities. For a medical physicist the principal advantage



is in the fact that a digital image can be considered a quantitative result with which it is possible estimate parameters or to perform measures.

In this short note we will discuss mainly of the x ray films, that are actually largely the more used detectors for radiography, and only briefly of the others detectors.

PRINCIPAL CLASSES OF X RAY DETECTORS

| Type | energy resolution | spatial resolution | efficiency | price |
|---|---|---|---|---|
| x ray films | no | very good | poor | low |
| screen-film systems | no | very good | medium | low |
| fotostimulable screens | no | very good | good | high |
| image intensifiers | no | good | high | high |
| scintillators | poor | no(poor) | high | medium |
| solid state | very good | no* | good | high |
| gas-filled detectors | medium | good | low+ | medium |

** actually there are attempts to construct position sensitive solid state detectors especially for those applications in which the energy sensitivity is very important as in angiography*

*+ the efficiency of such detectors is good in the energy range 1 ÷ 20 KeV but decreases quickly at higher energy; the efficiency is better using high pressure gasses .*

#### 1.2.1 The x ray film and the screen-film systems.

A radiographic film can be considered as a continuous (analogic) x ray detector, whose working principle is basically the same as for photography, i.e. the formation of a latent image through the interaction of the primary photons with the silver atoms. The subsequent development of the film, that is characterized by an amplification of the primary signal, produces a readable image. The efficiency of the detector is proportional to the linear absorption coefficient of the film and to the size of the silver bromine grains. A fast film characterized by larger size grains is more efficient; in the development this kind of film gives rice to large islands of silver, that it is possible to see by a microscope. This film is a low resolution one. The efficiency of a film is very small if compared with that of others x ray detectors; therefore the doses of radiation needed for a radiographic examination are proportionally bigger. The real advantage in using films is in the possibility to image a large area, in fact the film is the prototype of an "area detector". Before the last decade very few alternatives to the use of a film could be found, and in general they were characterized by poor resolution with respec to an x ray film. The storage capacity of a film is immense. Resolution for very fine grained film is about 4 $mm^2$; therefore, a 14"× 17" film contains about $4\times10^8$ pixels; a figure that must be compared with the actual capacity of a digital system that is about 1024×1024 pixels, i.e.$10^6$ pixels. In this sense we are far from the possibility of substituting the film in the x ray imaging of large area with high resolution. Obviously if a resolution of 100 $\mu m^2$ is enough (or we want image a smaller area) we can find excellent alternative to the film.

The process with which the visible image is formed by exposing the film to the radiation coming from the source and partially absorbed by the object can be schematized as follow: (i) a high energy photon impinging on the film remove an electron from one (or some) silver atom(s), giving rice to the local chemical reaction (reduction); so the number of silver grain that is transformed for unit film area is proportional to the photon fluence (photons/sec-mm$^2$) impinging on this area; (ii) during the development a reduced silver grain will form a small cluster of metallic silver with a controlled amplification process. At the end of this process it is possible to see a visible image.

A visible image can be physically represented by a two variable (x,y) continuous function; the physical meaning of this function is in general the point by point luminosity of the surface. It is well know that the luminosity depends from the external illumination, in order to avoid the problems arising by this fact it is useful to introduce a new quantity that can be more easily measured. The optical density (od) is a measure of the physical sensation of luminosity, it is defined by the point by point assorbance of a film illuminated with an uniform light source,

$$od = \ln\left(\frac{\Phi_0}{\Phi}\right) \qquad (20)$$

where $\Phi$ and $\Phi_0$ are the transmitted and incident light intensities respectively. In order to measure the optical density in one point of the film, it is possible to use a microdensitometer (figure 9). The film is sampled with a light pencil and the light transmitted is detected with a photomultiplier or a photodiode. The size of the light spot incident on the film can be reduced up to few square microns.

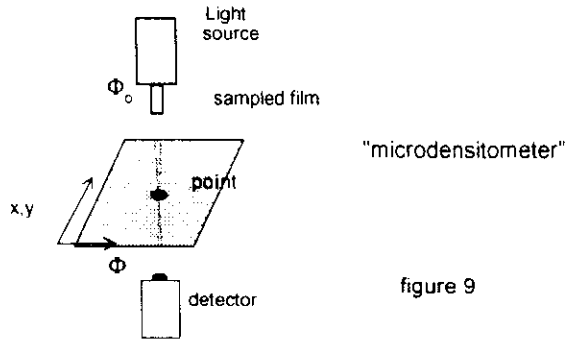


"microdensitometer"

figure 9

An optical density equal to one means that in that point only one tenth of the impinging light is transmitted. Therefore, greater the od is more black the point is. In the hypothesis of silver grains all of the same area ($\sigma$) uniformly distributed on the emulsion, the optical density can be considered as a function of the number of silver grains for unit surface (n) :

$$od = \sigma n \qquad (21)$$

If initially the number of silver grains is $n_0$ and the probability that an impinging photon would interact with a silver atom (P) is constant, the number of silver grains



reduced will be proportional to the x ray fluence, i.e. the number of photons for unit time and film area. Unfortunately the number of silver grains for unit area is not so large that all the photons impinging will have the same probability to transform a grain; in fact after n interaction the grain disposable to be transformed are $n_0 - n$. The probability of an interaction $\frac{dn}{dN}$ is proportional to the number of the grains capable to be transformed,i.e.,

$$\frac{dn}{dN} = k(n_0 - n). \qquad (22)$$

Resolving this differential equation it is possible to show that:

$$n = n_0(1 - e^{-kN}) \qquad od = od_0(1 - e^{-kN}) \qquad (23)$$

Where the second relation comes by the equation (21); this is the non linear response function of the film to a monochromatic radiation. In the case of a polychromatic photon beam one must consider that the probability of the interaction depends also by the energy of the photon. It is obvious that if the spectrum is constant it is possible to use the equation 23, and being the photon fluence related to the exposure (Ex) and to the dose, it is preferable to use exposure instead of photon fluence in the case of a continous spectrum. Rearranging the equation 23 one can be obtain the well known H&D (Hurter and Driffield) curve, i.e.,od vs the ln(Ex)

$$od = \gamma \ln(Ex) + b \qquad (24)$$

In fig.10 two H&D curves are shown, describing the sensitometric response of two typical film-screen combinations.

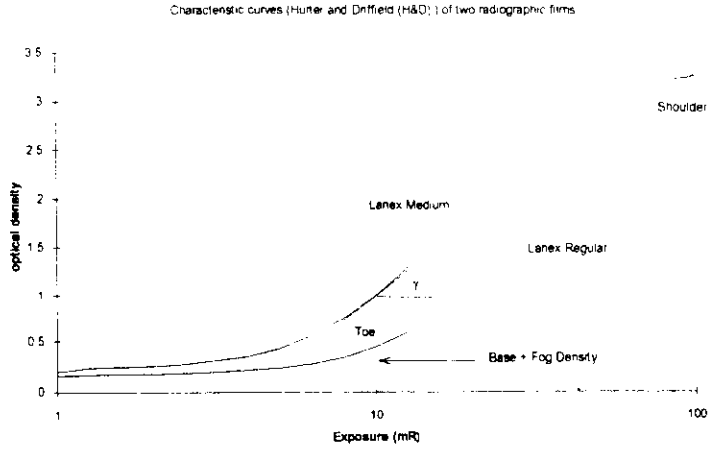


figure 10

This response function is characterized by several factors (i) the gamma ($\gamma$), (ii) the "fog" and the base od, (iii) the latitude. The gamma is the value of $\gamma = \frac{d(od)}{d\ln(E)}$, it can be defined as the maximum slope or as the average slope between two designated density values (0.25 and 2.0). Usually the $\gamma$ is about constant in an exposure interval of one order of magnitude. The fog is the shift toward higher od values of

sensitometric curve that can't be avoided: in fact in each film area some silver atoms are randomly transformed for many reasons, for example an unwanted pre-exposition of the film to light gives rice to an higher value of the fog. It is worth while to remember that the films must be kept in the refrigerator before the exposure. The film in fact works as counter, working on an integral mode, it means that; it sum the exposures in the time. A pre or post- exposition of the film limits its performances, because some silver grains are already reduced.

The dynamic (linear) range of an x ray film is the exposure range in which the sensitometric curve is linear; changing the film characteristics, the size of the silver grains, the superficial density of the grains etc., it is possible to extend and shift the sensitometric curve linear range. This range takes also the name of film latitude. The corresponding od range is almost fixed by the readability of the film; it is usually in the range 0.8-2.5 od units. Therefore the $\gamma$ assumes the meaning of a real measure of the performances of a film; in fact a smaller $\gamma$ indicates a larger sensitivity and, usually, a lower dose for the patient in order to get a well contrasted image. The use of a fluorescent screen is a very common trick to increase the sensitivity (and the $\gamma$) and so to reduce the patient dose.

The sensitometric curve can be determined experimentally using a step wedge, or a sensitometer, i.e., a system which is capable to expose the film to light flashes of wanted intensity. Measuring the optical density in the film area exposed and plotting the values vs the given intensities, one obtains the sensitometric curve and can determine the latitude and the $\gamma$.

figure 11

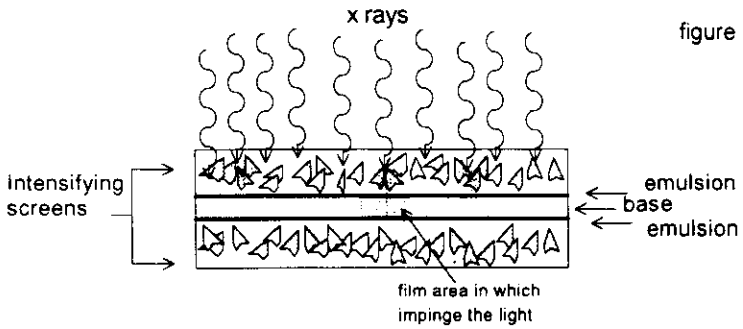


The major drawbacks of the films are in the low efficiency and in the low time resolution. For avoiding the first problem actually the film are not used by alone but with the interposition of a suitable phosphor, i.e. of a radiographic screen, see figure above. The concept is very simple. The film, that is sensitive to the light, is enclosed in two screens; the x rays impinging on the screen produces light during the interaction of primary x rays exposing the film and giving rise to the latent image. The interaction of x rays happens in the screen which is more absorbing than the film. The technique of the film-screen systems is actually the more used in radiography; in fact it offers a very good price/performances ratio with respect to the conventional films; these systems, despite of the fact that spatial resolution is worse, lead to a reduction of the patient dose, due to the larger efficiency.

Unfortunately,the low time resolution of the film and film-screen systems can't be avoided; in fact the only possibility to use a film in a dynamic study is to expose



several films in a short interval of time. This can be done, and was done in the early times of angiography, but with severe limitations and high costs. Practically the films and film-screen systems can be usefully used only for static studies.

In conclusion the most important characteristics of this class of detectors are the spatial resolution and the possibility to produce x ray images of large objects.

1.2.2 Image Intensifier- TV systems.

The X-ray image intensifier (XRII) is a device which uses electron optics in order to provide a image brighter than that gettable with a conventional intensifying screen. It was commercially available since 1950 and has been used intensivelly mostly in real time diagnostic procedures such as angiography.

The XRII is a complex detection system composed essentially by a vacuum cylindrical tube in whose concave inner front surface there is a scintillation layer and a suitably shaped photocatode. The electrons emitted by the photocatode are focused on a output flat phosphor screen (about 2 cm diameter) placed on the rear surface. The input diameter is 15 ÷ 35 cm; the image on the output screen can easily be seen by a TV camera .

The fact that the image formed on the input is about hundred times bigger than that on the output, and the high kinetic energy of the photoelectrons impinging on the output screen, are the reasons for the high brightness of the XRII. The brightness of the output image (for a given X-ray beam), known as conversion factor (CF), is the ratio between the luminance ($Cd/m^2$) and the exposure rate ($R/s^{-1}$)

$$CF = k\, n_s\, n_p\, n_o\, (m_f)^2\, V\, 10^7 \ (Cd.m^{-2}/R.s^{-1}) \qquad (25)$$

where k is a proportionality constant, $n_s$ is the quantum efficiency of the primary scintillation layer (i.e. the number of photons produced per X-ray photon), $n_p$ is the efficiency of the photoemissive layer (electrons/photon), $n_o$ is the efficiency of the output phosphor (photons/electron), $m_f$ is a linear reduction factor of the image intensifier, V is the image intensifier anode voltage. For example 3.000 60 KeV photons generate 100-200 electrons on the front phosphor, which, accelerated by 30 KV field, in turn produces about $2 \times 10^5$ photons.

The phosphor of the input screen (usually CsI) have a high quantum detection efficiency, good contrast and high resolution capabilities. On the rear phosphor (ZnS:CdS:Ag) a visible image is produced, that can be easily seen by the eye as well as by a TV camera and by photographic films.

In the beginning the XRII systems were not used in sophisticated imaging procedures because the XRII give rice to some aberrations. Actually with digital computers and fast electronic systems it is possible to correcte the image on line .

Typical resolution of a XRII is between 3 and 5 line pairs/mm measured at the input of the intensifier; the time resolution is ~1/30 seconds.

In figure 12 a digital radiographic system based on a image intensifier is shown; the image is catched on line with a TV camera and sent to the computer through a logarithmic amplifier and an ADC (Frame Grabber). The image can be visualized in a ordinary monitor an, simultaneously recorded in a video terminal recorder (VTR). The digitalized images are stored by the computer in hard disks or optical disks, and transmitted to other computers.

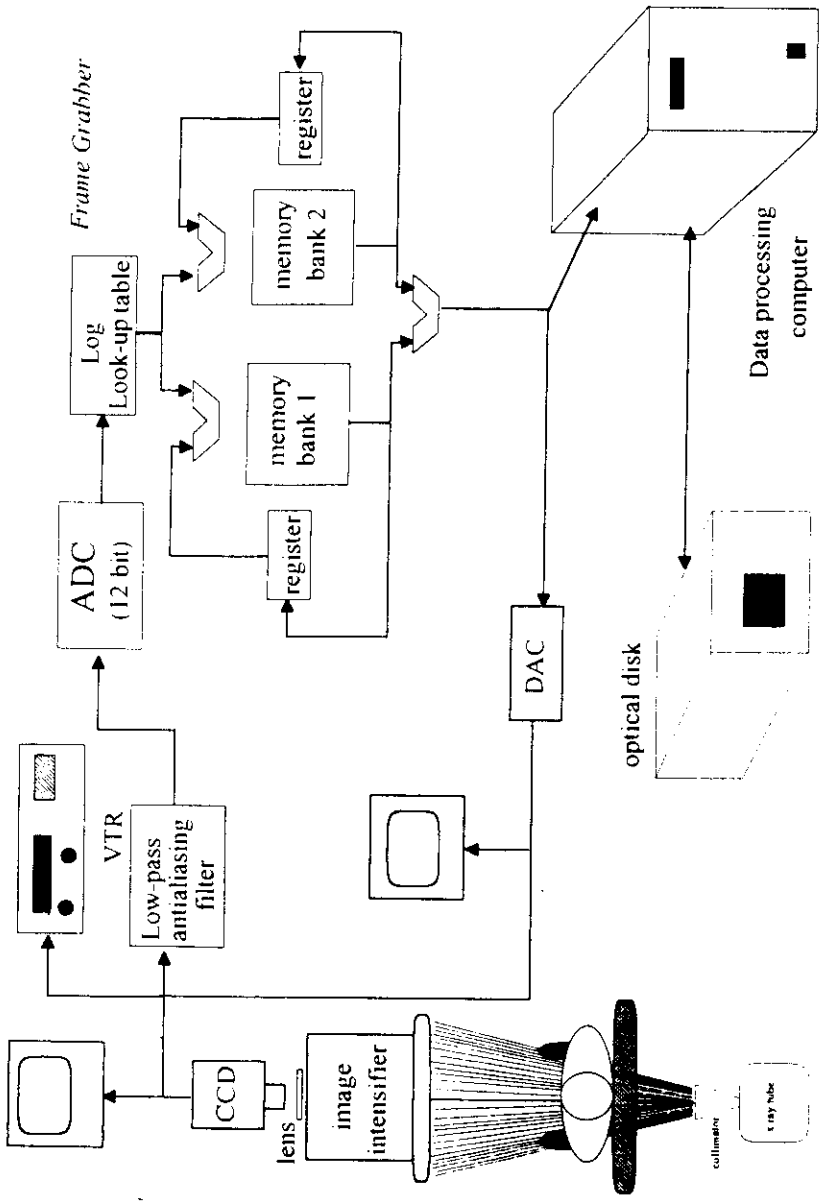


Figure 12 - Schematic view of a digital radiographic system based on an image intensifier coupled with a TV camera and a Frame



## 2 PHYSICAL FOUNDATIONS OF RADIOGRAPHYC SCIENCES.

The basic assumption that one makes in production of an image using the x rays is that the photons cross the imaged object following rectilinear lines. This means that the refractive index for the x rays is one, that is reasonably true in a first approximation. We assume in addition that, traversing the object to be imaged, only a part of the original number of photons is absorbed and that the removal of the photons from the beam is due only to the interactions with the object atoms. With these assumptions the probability of interaction for unit length, i.e. the linear absorption coefficient μ, is constant. In this case we can write the well known equation of absorption:

$$N = N_0 \, e^{-\mu x} \tag{1}$$

μ dx is the probability of an interaction in the path dx, such as dμ x is the increment of probability due to the a μ change; μ depends by the density ρ and elemental composition of the sample:

$$\mu x = \frac{\mu}{\rho}\rho x = \frac{\mu}{\rho}m \tag{2}$$

where $\frac{\mu}{\rho}$ is the mass absorption coefficient and m is the mass for unit surface of the sample.

One useful concept is that the mean free path of the radiation in a uniform material is the inverse of linear absorption coefficient ,

$$\bar{x} = \frac{\int_0^\infty x \, e^{-\mu x} dx}{\int_0^\infty e^{-\mu x} dx} = \frac{1}{\mu}, \tag{3}$$

in fact the probability that the path would be x is equal to $\frac{N}{N_0} = e^{-\mu x}$. Knowing the approximate composition (the matrix) and the density of the object to be imaged we can calculate the mass absorption coefficient and the linear absorption coefficient and to deduct mean free path of the x rays of a given energy. It is useful to note that the thickness $\mu^{-1}$ is that at which the intensity of the beam is $e^{-1}$ of the original one.

### 2.1 Radiographic Imaging and the Absorption Coefficients.

A very simple way to produce an x ray image is to perform a single projection obtaining a linear projection or an area projection (figure 13). Geometrical considerations, used also in the geometrical optics, lead to the conclusionthat the source can be modelled as a point source if the source and the detector distance is » than the source diameter. If this approximation can't be applied the source is extended. When we consider a point source approximation we speak about a fan beam; when the source is extended we speak of a parallel beam (see figure 12). An x ray tube can be considered in general a point source, being its emitting area > 10 mm² for an ordinary x ray tube and > 0.5 mm² for a microfocus

An interesting problem to consider is the divergence of the beam and its brightness. The brightness of a source is the intensity emitted by one small area dS of source in the unit solid angle in a given bandwidth. A small divergence source, like a laser, is in general characterized by an high brilliance, because the beam is concentrated in a small solid angle. This occurs also for the Synchrotron Light (SL) that is characterized by an high brightness and a small divergence of the beam. An high brightness low divergence source can be considered, as in the case of SL, a parallel source rather than a point source. In figure 14 the brightness of a x ray tube is

compared with that of actual and future SL sources; several orders of magnitude in brightness have been gained. The use of such x ray sources would be restricted to those problems in which an high brightness and small divergence of the beam are mandatory, as in the microanalyses or in microtomography in which a small object is analyzed with a very high spatial resolution. To use this source in the imaging of big objects is not in general simple and useful.

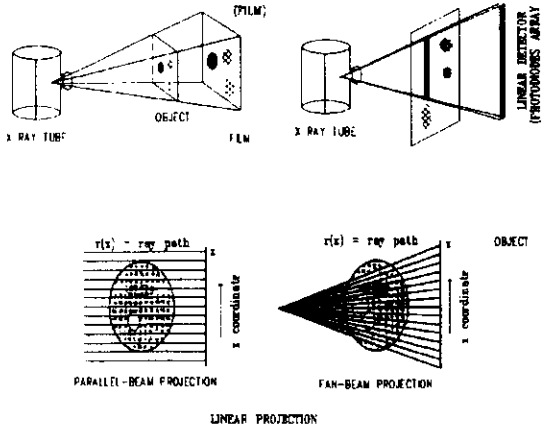


figure 13

One problem with the image obtained with a single projection is the formation of the penumbra when the source is extended; in fact, as clearly shown in figure 15 b, the projection of a point placed at a distance h' between the source and the detector (film) has a diameter $\Delta P$ given by:

$$\Delta P = \frac{(h-h')}{h} \qquad (4)$$

Obviously the penumbra disappears when the object is placed on the film, and is very thin; unfortunately, this latter approximation holds rarely in the case of medical radiography. An object imaged with a fan beam geometry is magnified h'/h times; this occur also in the tomographic techniques using fan beam. The use of a parallel beam can be done only using well collimated position sensitive detectors. In fact, the image produced with a parallel beam without collimator is completely degraded by the presence of the transverse rays (any point in an extended source can be seen as a point source). In tomography parallel beam geometry is in use (with a narrow collimation of the detectors), whereas in radiography this case is very rare.

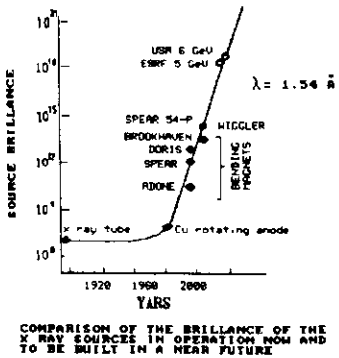


Figure 14



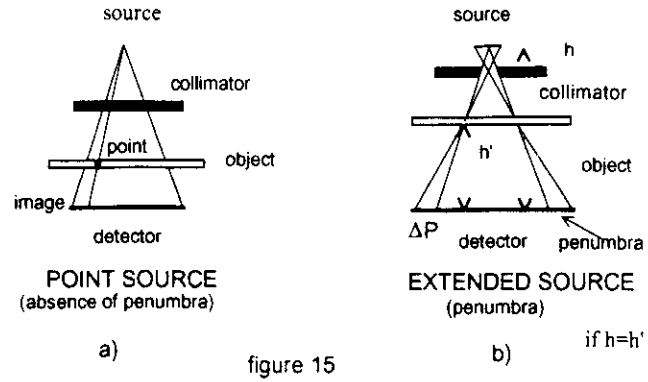


figure 15

In the case of a single projection (see fig.13) the process of formation of the image of a three dimensional object can be schematized as follow. Let $\mu(x,y,z,E)$ be the linear attenuation coefficient point by point in the object, it represent the capacity of the object to absorb photons of a given energy (E) and let N(x,y) be the number of photons impinging on a point of the detector surface. N(x,y) is given by:

$$N(x,y) = N \int_{\vec{r}} e^{\mu(x,y,z)l}\, dl \qquad (5)$$

In the above equation the integral is along the x ray path $\vec{r}$ (see figure 16), that in the case of a fan beam is a transverse line. At the end of this process the image we obtained is a two dimensional representation (N(x,y)) of a three dimensional object, this means that we have lost something. In particular, the integral along the line implies that we lose the information about the changes of $\mu$ along the path. In this simple image formation model we can assume that one x ray path $\vec{r}(x,y)$ correspond to one point in the area detector. Therefore the response function of a radiographic system can be written in a first approximation

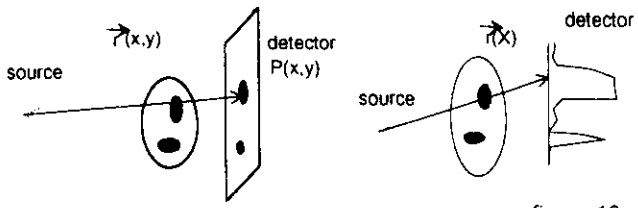


figure 16

$$N(x,y) = N_0\, e^{-\bar{\mu}\,\vec{r}(x,y)} \qquad (6)$$

In the above equation we make the assumption that $\vec{r}$ is the path length inside the object and $\bar{\mu}$ is a mean absorption coefficient along the ray path.

Unfortunately with a single projection we are not able to discriminate a variation due to a change in thickness or in density from another one due to change of mass

absorption coefficient. In fact a variation of density can masks a variation in thickness and composition and vice versa (figure 17). This is a severe restriction for the single projection radiography; read only the advent of the tomographic techniques have partially removed these limitations.

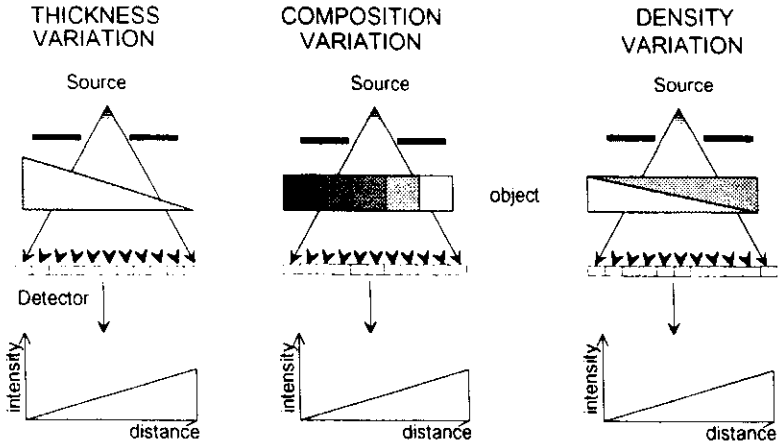


Figure 17

2.1.1The Mass Absorption Coefficients.

The mass absorption coefficient $\frac{\mu}{\rho}$ depends only from the elemental composition of the examined sample and from the energy of the incident photons. This coefficient can be divided in three parts which are related to the major interactions that take place during the passage of a photon beam of energy less than 100 KeV through a sample (see fig.18); in this energy range the annihilation processes don't exist). That interactions are the photoelectric, Compton (or incoherent) and Rayleigh (or coherent) scattering. The dependence of these three parts of the mass absorption coefficient from the atomic number of the sample and from the energy of the photons can be approximately written as follows:

$$\frac{\mu}{\rho} = 20.64\, E^{-3.28}\, \bar{Z}^{4.62} + \sigma_{KN}(E)\, \bar{Z} + 2.8\, E^{-2.02}\, \bar{Z}^{2.86} \qquad (7)$$

where $\sigma_{KN}(E)$ is the Klein-Nishina cross section and $\bar{Z}$ is the effective atomic number of the sample (Rutherford ed. al., 1975). These formula shows as the dependence from the energy and from the atomic number of the photoelectric part of the coefficient is stronger (3.24 and 4.62 respectively) than that of coherent and incoherent scattering. This means that the decrease of this contribution is proportionally more rapid than that of the other two terms. In this sense we can speak about one energy range in which the photoelectric scattering is dominant and one, at higher energy, in which the incoherent scattering is dominant. In Figure 19 the linear absorption coefficients for soft tissue (muscle), fat and bone are reported as a function of photon energy. It is evident that in the energy interval 20 ÷ 40 keV the differences are large[4], but the coefficients are still so high that the mean free path is ~ 5 cm, that is

[4] Consequently also the radiographic contrast, that is proportional to the difference of the linear absorption coefficients, is larger.



not so large to allow the photons to pass easily through the human body. In figure 20 the mass absorption coefficient of a contrast media is compared with that of water; the very large difference in the mass absorption coefficients that can be obtained shows as it is possible to visualize with a high contrast the vessels in which the contrast media is concentrated.

When we study the absorption by a sample of a polychromatic photon beam we should take into account the changes with energy of the mass absorption coefficients. The response function of an absorptiometric technique in this case change as follows:

$$N(x,y) = \int_0^\infty N_0(E)\, e^{-\vec{\mu}(E)\,\vec{r}}\, dE \qquad (8)$$

Where the integration is carried out on the whole source spectrum ($N_0(E)$). It is in general cumbersome to study the response function of absorptiometric technique considering the effect of polychromaticity of primary radiation, therefore it is considered an acceptable simplification to represent the primary beam with an effective energy, for example the mean energy:

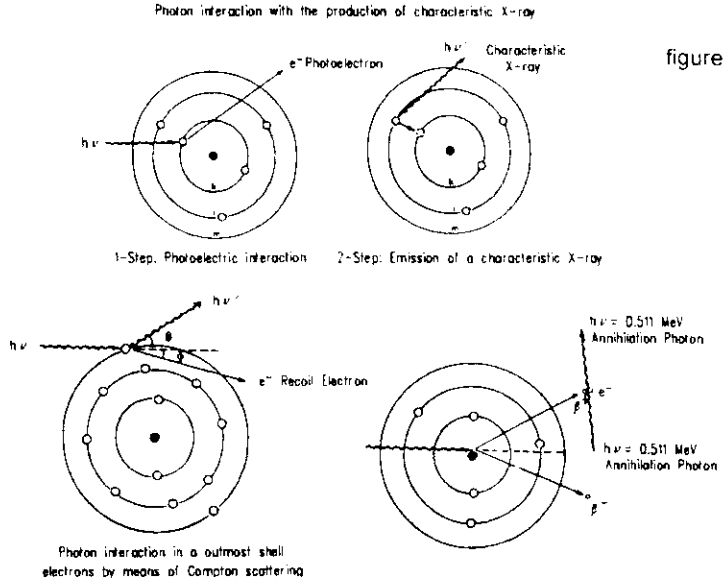


figure 18

$$\bar{E} = \frac{\int_0^\infty E\, N_0(E)\, dE}{\int_0^\infty N_0(E)\, dE} \qquad (9)$$

This simplify the formalism, but does not underline adequately effects that are in general related to the fact that the primary spectrum (e.g., the spectrum of x ray tube) and the detected spectrum (i.e., that impinging on the area detector) are different. This effect is referred to as beam hardening; in fact the detected spectrum is more rich of high energy photons than the primary one. In order to eliminate the influence of this effect we should use an energy dispersive detector (such as a solid state detector), but this is in practice impossible. It is useful to remark that the

influence of this effect is very strong if we attempt to correlate absorption measurements made on samples with large changes in composition. This effect can be in general neglected in medical radiography because in this case the variation of μ are very small.

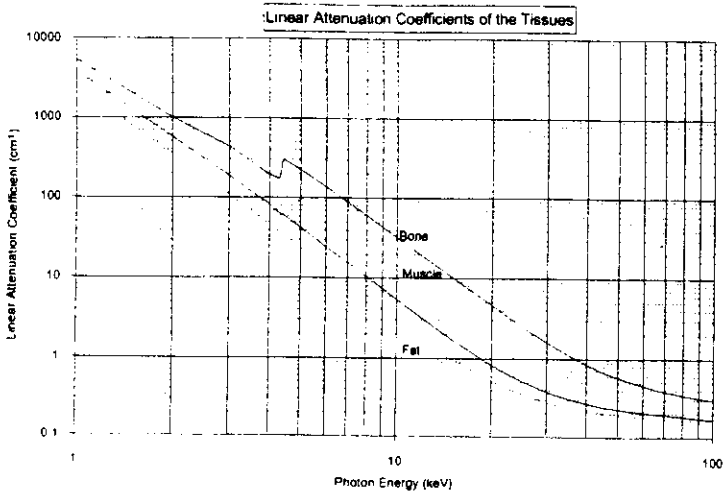


Figure 19 At lower energies, the photoelectric effect is more dominant, making the mass attenuation coefficient of the bone higher than that of the muscle which in turn is higher than that of fat. At higher energies, the incoherent scattering is more dominant, making the mass absorption coefficient of these tissues approximately equal; the differences are almost completely due to the different densities of tissues.

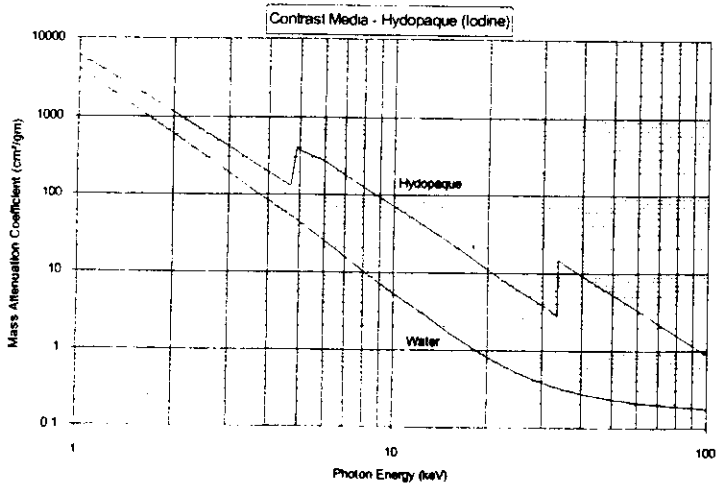


Figure 20 Comparison of the mass absorption coefficients of water and a contrast media (Hydopaque)



## 2.2The Response Function of Absorptiometry

When we look at a radiographic image, that is a distribution in the plane x,y of the luminosity, some questions instinctively arise: (i) how I can define the minimum detectable luminosity variation, (ii) what is the luminosity threshold, i.e.. the minimum detectable signal, (iii) how the luminosity of two near point are correlated, etc.

To start with the answers we should define what we measure; in the case of a radiographic film the measured quantity is the optical density, in that of a image intensifier-TV systems the output voltage from the camera, etc., but it is self evident that in any case the physical quantities that we measure is the intensity distribution (or the number of incident photons in each detector element or in unit area element of the detector). To approach the not easy subject of the detectability of one defect in an image it is needed to fix the limits of our considerations. We are interested to the detectability in a physical sense, therefore we will not speak about the ability of our eye to detect a particular defect in an image.

In order to fix some concepts it is useful to study the response function of an absorptiometric device, as a function of photon energy, sample thickness and composition. The extrapolations from a single absorptiometric system to a system using an area detector or a position sensitive detector are straightforward. Obviously this is true for an ideal device, but not for a real one in which, passing from a well collimated single source-detector device to a multiple detector (or area detector system), many problems like the contribution of the scattering or the cross-talk between the detector elements became very important. In our consideration we will neglect these aspects that can more easily treated with the optical system theory.

The number of photons detected, such as that emitted by the source, follow the Poisson distribution, therefore some useful deductions can be done using the properties of this distribution and some simple statistical considerations.

### 2.2.1Statistical Considerations

Let us consider to a parallel beam, in order to simply the formalism, and let start with the case of an uniform sample or a sample surrounding a defect (i.e., a zone with a different linear absorption coefficient).

If the object can be modelled as an uniform sample, it is possible to measure its linear absorption coefficient knowing its thickness (L) (conversely, knowing its mass for unit surface, we can calculate its mass absorption coefficient). If we measure the μ's of two samples we can be curious to know what is the smallest variation of detected counts (N) that we can appreciate. The answer is immediate if we follow a simple statistical approach. We can consider that the difference $\Delta N = N - N'$ is statistically significant if:

$$N > N' + b\sqrt{\sigma^2(N) + \sigma^2(N')} \qquad (10)$$

where $\sigma^2(N)$ is the variance of N and b (= 1,2,3) can be chosen according to the uncertainty level that is satisfactory for our approach. The detected counts follow a Poisson distribution, consequently a good estimation of the variance is N and the equation 10 can be written also as:

$$N' > N + b\sqrt{N' + N} \quad \text{if } N' \approx N \Rightarrow N' > N + \sqrt{2N} \qquad (10')$$

If we know the response function ( f(x)) of the measuring system which links the quantity x that we want estimate to the quantity f(x) that we measure, the resolving power for the quantity x is given by the following relation:

$$\Delta x = \frac{b\left[\sigma^2(f(x_1)) + \sigma^2(f(x_0))\right]^{\frac{1}{2}}}{\frac{df(x)}{dx}} \qquad (11)$$

where $\sigma^2(f(x))$ is the calculated variance of the measured quantities and $\frac{df(x)}{dx}$ is the sensitivity. If we can assume that the two measured quantities $f(x_0)$ and $f(x_1)$ have the same variance the above equation becomes more simple:

$$\Delta x = \frac{b\left[2\,\sigma^2(f(x))\right]^{\frac{1}{2}}}{\frac{df(x)}{dx}} \qquad (12)$$

If we measure only one time the quantity f(x), but we know its distribution (as in the case of detected photons) we can estimate $\sigma^2(f(x))$ from the distribution.

An application of these concepts is the measure of a linear absorption coefficient of material by measuring the number of photon that pass through a sample of thickness L (see fig. 21). Making the derivative of equation 1 we find the sensitivity,

$$\frac{dN}{d\mu} = -L\,N \qquad (13)$$

Therefore the minimum μ variation that we can detect, i.e. the resolving power, is:

$$\Delta\mu = \frac{b\sqrt{N'+N}}{LN} = \frac{b\sqrt{2}}{L\sqrt{N}} = \frac{b\sqrt{2}\,e^{\frac{\mu L}{2}}}{L\sqrt{N_0}} \qquad (14)$$

where $N_0$ is the number of photons incident on the object surface. By the last equation it is possible observe that the minimum detectable Δμ increases with the object size (L), i.e. with a thicker object the measure system becomes less sensitive.

2.2.2 Contrast and Contrast Ratio and Signal to Noise Ratio.

In order to discuss the more complex case of a position sensitive detector (or an area detector), let us consider the case of a small object of thickness dl placed inside an uniform sample (for example a thin piece of Teflon in a beaker filled with water). If we take a single linear projection of this object we will obtain a result very similar to that shown in figure 21.

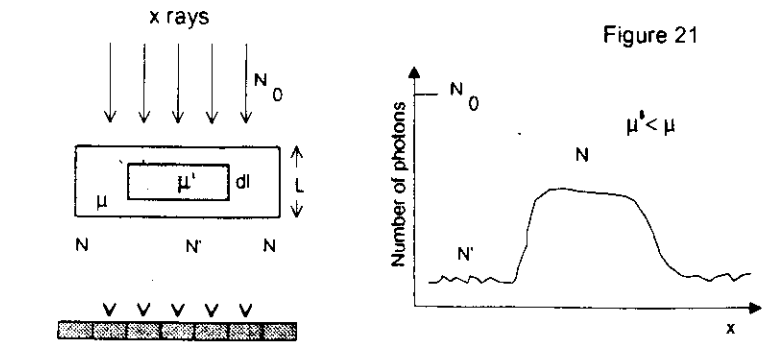





Figure 21

L : sample thickness
dl : defect thickness



The difference ΔN = N - N' between the counts in a detector element inside the defect (N) and outside it (N') is the contrast and $\frac{\Delta N}{N}$ is the contrast ratio. Observing the detected profile you can note that the counts N(x) don't reproduce exactly the edge; this is due to the limited resolution of our measuring system. It is easy to image that if contrast is very low the small object becomes invisible.

The equation 14 can be still used also in this case considering that the measured quantities are N and N' taken in the central part of the small object and in one side of the sample respectively, in order to avoid that part of the measured profile near the surface of the object. Also in this case it is possible to assume that the variance of measured photons is N. The minimum detectable contrast is

$$\Delta N_{min} = b\sqrt{N+N'} \approx b\sqrt{2N} \qquad (15)$$

Let us now rewrite ΔN = N - N' and N/N' in a different manner:

$$\Delta N = N'(e^{\Delta\mu dl} - 1) = N(1 - e^{-\Delta\mu dl});\ N = N'e^{\Delta\mu dl} \qquad (16)$$

where μ' is the absorption coefficient of the object and $\Delta\mu = \mu - \mu'$ is the difference between the linear absorption coefficients of the sample and the small object inside it.

The sensitivity to a Δμ variation is given by:

$$\frac{d\Delta N}{d\Delta\mu} = N'\,dl\,e^{\Delta\mu dl} = N\,dl \qquad (17)$$

Therefore the sensitivity depends directly from the defect size dl and it decreases with the object thickness (L), because N decreases with L.

Therefore the minimum detectable $\Delta\mu_{min}$ is:

$$\Delta\mu_{min} = \frac{b\sqrt{N+N'}}{dl\,N} \approx \frac{b\sqrt{2}}{dl\sqrt{N}} \qquad (18)$$

It worth while note that the sensitivity and the minimum detectable $\Delta N_{min}$ or $\Delta\mu_{min}$ depend by L. It means that is harder to detect a defect inside a bigger sample. This severe limitation can be overcome only using the tomography; if we take L=0 in the equation 16 and 18, i.e., if we neglect the effect of the size of the sample around the object to be detected, we obtain two relations valid for tomography and we can immediately note that the contrast ΔN is greater. In tomography the quantity that is reconstructed is the map of linear absorption coefficients μ(x,y) that is calculated using the profiles measure at different angle around the sample. The equation 18 is still valid if we consider that each ray sum can be decomposed in m pixel of length dl (L = m dl), therefore the average of the counts in a ray sum are $N_D$ = m N, where N is the average of counts for each pixel; substituting $N_D$ in equation 18 we obtain the following relation:

$$\Delta\mu_{min} = \sigma(\mu) = b\frac{\sqrt{2m}}{dl\sqrt{N_D}} \qquad (19)$$

This relation is very similar, apart the terms depending from the reconstruction algorithm, to that deduced by many authors. Our deduction clearly show that one of the advantages of the tomography is in the decrement of the minimum detectable Δμ or in other words in an increment of the contrast. Another advantage is that the dl in the tomography is chosen "a priori", consequently we can more easily optimize the

contrast, increasing or decreasing the exposure (and the dose) at the desired level.

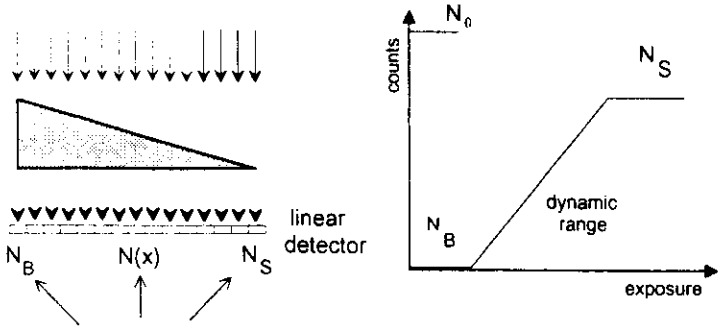


figure 22

Let us assume that μ and L constants and let change only μ' and dl, in this case the contrast can be written as:

$$\Delta N = \frac{d(\Delta N)}{d\mu'} \Delta\mu = N\, dl\, \Delta\mu \qquad (20)$$

at the same ratio one can arrive considering in equation 16 that the exponent $\Delta\mu_{min}\, dl_{min}$ is small and taking only the first two terms of the expansion $(1+ \Delta\mu_{min}\, dl)$ The contrast ΔN depends mainly from the number of photons that have been counted during the measure (N), therefore the minimum detectable $\Delta\mu_{min}$ and the minimum detectable defect size ($dl_{min}$) are inversely proportional. In fact it is possible to detect a very thin defect, only if the Δμ is large, i.e. the material or the density of the small defect and that of the surrounding sample are very different . To detect smaller defects we should increase the contrast, for example increasing the statistic or increasing the Δμ, choosing an energy in which the μ' difference between the surrounding sample and the defect is larger.

The signal to noise ratio can be written as follow:

$$SNR = \frac{N-N'}{\sqrt{N+N'}} \text{ if } N \approx N' \Rightarrow SNR = \sqrt{\frac{N}{2}}\,(e^{\Delta\mu\, dl} - 1) = \sqrt{\frac{N}{2}}\,\Delta\mu\, dl \qquad (21)$$

This relation can be demonstrated in many different ways, such as in the theory of the contrast-detail curvesw (Rose theory).

A deduction that one can do from the above equation is that one can decrease $\Delta\mu_{min}$ at will, exposing the object for a longer time. Can this be true? obviously not. What is inexact in our model to arrive to these wrong conclusion? nothing of really unrecoverable, we have forget that our system, as all real measuring systems, is characterized by a dynamic range and by a background ($N_B$). In particular, as clearly shown in figure 19 there are two limits in the total counts for unit detector area that the measuring system can detect, the background $N_B$ and the saturation $N_S$ counting rates. $N_B$ is the minimum amount of counts per unit time that are in any case detected, which origin can be scattering in the sample or noise in the detector; $N_S$ is maximum number of counts per unit time that the system can detect. If an higher flux of photons reaches the detector the counts will fluctuate around the $N_S$ value. The equation 18 is therefore valid only in the range $N_B < N < N_S$ and the dynamic



range of the measuring system is $N_S - N_B$. Using an x ray film the dynamic range coincides with the od interval in which the response function od vs log(Ex) is linear, at the margins of this interval the od still increases or decreases with a smaller γ. In this sense the film is a more reliable detector, because it continues to work also outside the margins of the dynamic range; conversely there are some detectors that suddenly stop to work outside this range. Is frequent to see radiographic films that are overexposed or underexposed but that can be read, even with some difficulties. When we speak about the need of a wide dynamic range in the ray radiography, we implicitly refer to the fact that is not easy to match the dynamic of X-rays impinging on the detector with the detector dynamic range. Let suppose that we have to study the energy of primary beam or the thickness of the sample that we can image with a high contrast; in these cases we are interested to a relation that give the maximum $\Delta\mu_{min}$ as a function of the sample μ and thickness L. In we want know the optimal thickness of the sample for a given sample μ. This can be easily done using the equation 14 and putting the derivative equal to zero, the result is very simple and attractive:

$$\frac{d(\Delta\mu)}{dL} = \frac{b\sqrt{2\, e^{\mu L}}}{\sqrt{N_0}}\left[\frac{2-\mu L}{2L^2}\right] = 0$$

$$L_{opt} = \frac{2}{\mu} \qquad (22)$$

The same things can be done for the equation 18 deriving for the defect size dl and arriving to the conclusion that

$$dl_{opt.} = \frac{2}{\Delta\mu_{min}} \qquad (23)$$

fixing thus the minimum defect size that can be observed for a given Δμ. This relation is very attractive because fix an inverse proportionality between the theoretical spatial resolution and the $\Delta\mu_{min}$.

In conclusion, studying the response function of an absorptiometric system, it is possible to optimize the parameters of the radiographic system in order to maximize the contrast and minimize the size of the smallest detectable object. It is necessary underline that some of these parameters can't be changed in regular medical systems (e.g., the path length of the beam inside the body that is fixed by the body size). This is not true in general and the new revival of microradiographic and microtomographic techniques shows which are the potentialities of the absorptiometric techniques when you can optimize simultaneously all the parameters.

The procedure to find the optimal parameters set it is very easy in the case of a single energy system but can be more cumbersome for dual energy absorptiometers or for CT systems. The most interesting part of these studies are usually the optimization of the primary(-ies) beam energy. In order to correctly place the question we should stress that there are many problems that you can solve using an absorptiometric system. Using an absorptiometric system it is possible to determine the density and the elemental composition of the examined sample, and also to measure thickness (or better thickness variations), assuming that the sample is homogenous (this kind of measurement are more frequent in quality control in industry). How it is possible to determine the optimal conditions in order to determine such quantities? The answer in essentially in the dependence of μ from the quantity we want measure. In particular, it worth immediately recall that the mass absorption coefficient of a

particular element $(\frac{\mu}{\rho})_i$ is the sum of the three partial coefficients: photoelectric, incoherent (Compton) and coherent. The dependence from atomic number and energy of these coefficients is strongly different (see equation 7). In particular, the photoelectric coefficient is dominant in the low energy range, whereas the Compton one is dominant at higher energies. The dependence of the Compton coefficient from Z is about linear, therefore in the energy range in which this interaction is dominant the dependence of $\mu$ from Z is weaker than in the energy range in which the photoelectric interaction is dominant. All these statements are well known to the people working with rays. We can conclude that in order to optimize the energy we should find the energy of the primary beam that maximize the $\Delta\mu$ between the two parts of our object we want discriminate. This task is very simple because if we know roughly the composition of the particular we want observe and that of the surrounding tissue we can choose that energy for which the $\Delta\mu$ is maximum. It worth stress that we should maximize $\Delta\mu$ and not $\Delta(\frac{\mu}{\rho})$ because several times the major contribution to the change is due to density more than atomic number variations. Unfortunately, working with radiography we can't do this simple procedure because we must take into account also other significant parameters, such as the object size.

A statement that it is easy to do is the following: if you want measure Z-variations you should use lower energy in order to increase the contribution of photoelectric part of mass absorption coefficient, if you want measure density variations is better to use higher energy in order to increase the Compton contribution. In practice you should found an useful compromise between the energy that optimize the counting rate and the energy that maximize the $\Delta\mu$, taking the object size as fixed.

### 2.2.3 DUAL ENERGY ABSORPTIOMETRY

The observed sample can be model in many cases as a two component mixture, like in the case of measurement of Bone Mineral Content (BMC). In this case holds a simplified model in which the central region of one object is composed of a mixture of two components: (i) a completely mineralized tissue having a higher Z and (ii) the soft tissue. This central region is surrounded by soft tissue. The problem is more or less the same as before in which a small defect was surrounded by an uniform object. In this case the problem is to find the weight fraction of bone in the central region. This is a typical problem that can be solved with an absorptiometric measure. It is convenient to approximate the $\mu$ of the central region as follow.

$$\mu = \mu_{st}\, w_{st} + \mu_{bm}\, w_{bm} \tag{24}$$

where $\mu_{st}$ and $\mu_{bm}$ are the absorption coefficient of soft tissue and mineralized tissue, respectively, and the w's are their weight fractions. It is necessary to impose the condition that $w_{st} + w_{bm} = 1$

Now we perform two independent transmission measures using different primary energies, for example at one energy in which the photoelectric dominates and at one in which the incoherent scattering (Compton) dominates. Thus it is possible to write two independent absorptiometric relations:

$$\ln\left(\frac{I}{I_0}\right) = (\mu_{st}\, w_{st} + \mu_{bm}\, w_{bm})L \tag{25}$$

$$\ln\left(\frac{I'}{I'_0}\right) = (\mu'_{st}\, w_{st} + \mu'_{bm}\, w_{bm})L$$



where $I_0$ and I are the incident and the transmitted intensities in the first measure (with a lower energy beam) an $I'_0$ and I' are the corresponding intensities in the second measure. Solving the system of two equations for $w_{bm}$ we obtain:

$$w_{bm} = \frac{\mu'_{st} - k\mu_{st}}{k\Delta\mu - \Delta\mu'} \tag{26}$$

where $k = \frac{\ln\left(\frac{I_0}{I}\right)}{\ln\left(\frac{I'_0}{I'}\right)}$, $\Delta\mu = \mu_{bm} - \mu_{st}$ and $\Delta\mu' = \mu'_{bm} - \mu'_{st}$

It is evident that the precision with which it is possible to measure $w_{bm}$ depends from the statistical error on the measure of the intensities at the two energies. It is easy to observe that at the higher energy we have an higher counting rate, because the $\mu$'s are lower, but the intensity ratio is smaller, whereas at the lower energy happens the opposite. In practice, we detect the Bone Mineral with the lower energy and the higher energy measurement is used in order to correct for the bone thickness. Therefore, we can optimize the lower energy in order to measure the $w_{bm}$ and the higher energy to measure the bone size.

The real situation is more accurately depicted in figure 23, where the bone with a thickness dl is surrounded by soft tissues. In this case a more precise measurement can be done performing a linear transverse scan of the bone section. In this case we can use as reference, instead of the $I_0$ and $I'_0$, the intensities measured in that part of section in which the bone is absent $I_{st}$ and $I'_{st}$, for example at the two side of bone section (see figure 23). In this case the system of equations become:

$$\ln\left(\frac{I_{bm}}{I_{st}}\right) = (\mu_{st}\, w_{st} + \mu_{bm}\, w_{bm})\, dl \tag{27}$$

$$\ln\left(\frac{I'_{bm}}{I'_{st}}\right) = (\mu'_{st}\, w_{st} + \mu'_{bm}\, w_{bm})\, dl$$

This is what it is done in practice; for example to measure the Bone Mineral of a small size bone, as the case of the head of forearm, we can perform a scan at an energy of about 30 keV and another at 60 keV. In the case of spine, which is placed inside the trunk, which is ~ 20 cm long, the absorption is so high that higher energies are needed in order to optimize the measurement.

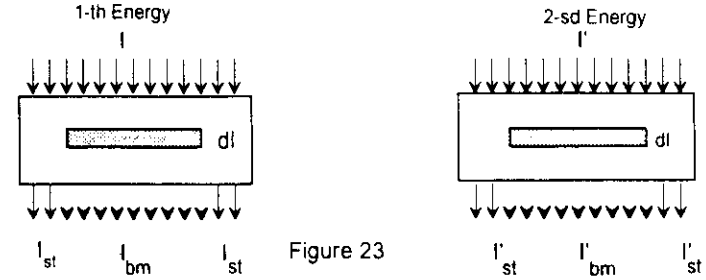


Figure 23

It is possible to make same consideration in the case of two white spectra obtained with two different KV and suitable filtration of the beam. This is done for dual energy tomography, using two mean energies, one that falls in the energy interval in which the photoelectric contribution is dominant and the other one in an interval

dominated by the Compton. This is actually a little more than an attractive prospective because the construction of a dual energy tomograph is a not easy job.

2.2.4 K-EDGE FLUOROSCOPY.

Another very interesting possibility, that is used in practice in the radiographic exams, is the use of a contrast medium, i.e. the injection in the observed object of a substance having an higher absorption than the object matrix. Assuming that the injected substance is concentrated in some parts (substructures) of the object we can display better the shape and the size of these substructure. This is done in particular for the artery, injecting in the blood circle an iodinated medium; this technique is commonly known as angiography. There are several problems with angiography especially if we attempt to perform dynamic studies. In fact, if we want detect the perfusion of the iodinated medium in the circle we must inject it instantly; also in this case, if we use only one energy it is not easy to determine the size of the vessels and of the obstructions (see fig.24). Now there are several attempts to perform angiographic studies using two energies, one above the K- absorption edge of the iodine and one below. In particular the use in this case of a synchrotron source is very attractive because you can produce two intense monochromatic beams very near the K-absorption edge, so we can completely observe the advantage of the discontinuity of the iodine linear absorption coefficient.

The K-edge fluoroscopy is the technique with which we can quantitatively determine the concentration of the contrast medium in a region of the observed object or the size of this region. In fact, if $\mu^T_1$ and $\mu^I_1$ are the linear absorption coefficients below the K-edge of the tissue and of the iodinated medium respectively, and $\mu^T_2$ , $\mu^I_2$ that above the K-edge, we can model these coefficients as follow:

$$\mu_1 = \mu^T_1 w_T + \mu^I_1 w_I \qquad (28)$$

$$\mu_2 = \mu^T_2 w_T + \mu^I_2 w_I$$

with $w_T + w_I = 1$

The two parts of the linear absorption coefficients are referred to the tissue (T) and to the contrast medium (I) respectively. Being the two energies very near we can assume that:

$$\mu^T_1 \approx \mu^T_2 \quad \text{and} \quad \mu^I_2 = \mu^I_1 + \Delta\mu_k$$

so $\mu_2 = \mu_1 + \Delta\mu_k w_I$

where the $\Delta\mu_k$ is the jump of the linear absorption coefficient at the K-edge.

We can so write the two following relations:

$$\ln\left(\frac{I_0}{I}\right) = \mu_1 \, dl \qquad (29)$$

$$\ln\left(\frac{I'_0}{I'}\right) = (\mu_1 + \Delta\mu_k w_I) \, dl$$

solving the system for the $w_I$ we obtain:

$$w_I = \frac{\mu_1}{\Delta\mu_k}\left[\frac{\ln\left(\frac{I_0}{I}\right)}{\ln\left(\frac{I'_0}{I'}\right)} - 1\right] \qquad (30)$$



$I_0$, as in the case of the dual energy, is the intensity detected passing trough a section conteining only soft tissue. In this case the first absorptiometric relation, taken at an energy below the K-edge, is used in order to correct for the thickness of the substructure with the contrast medium. The weight fraction of the iodine is determined using the second relation, i.e., that at an energy above the K-edge.

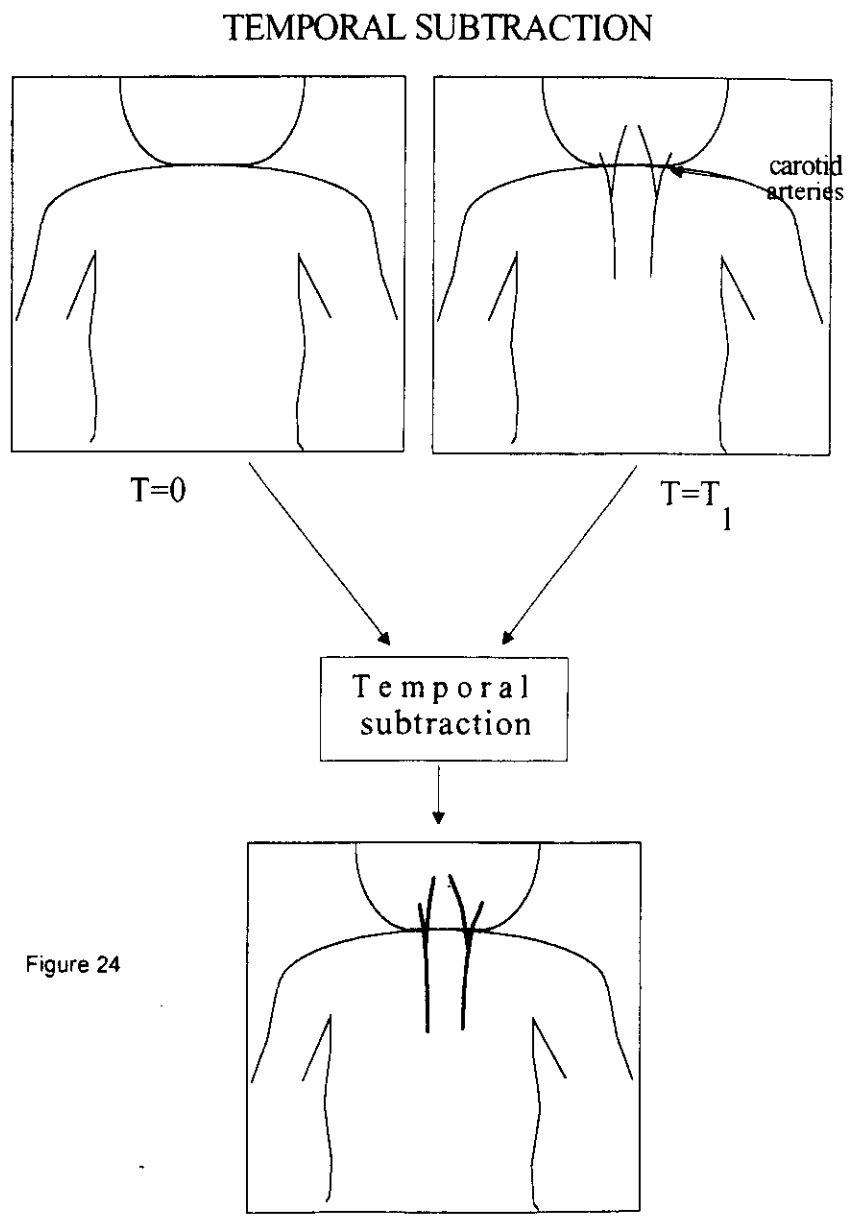


Figure 24